nature physics

SUPPLEMENTARY INFORMATION

DOI: 10.1038/NPHYS3895

One-dimensional spinon spin currents

Daichi Hirobe,[1,*] Masahiro Sato,[2,3] Takayuki Kawamata,[4] Yuki Shiomi,[1,2] Ken-ichi Uchida,[1,5] Ryo Iguchi,[1,2] Yoji Koike,[4] Sadamichi Maekawa,[2,3] and Eiji Saitoh[1,2,3,6,†]

[1]*Institute for Materials Research, Tohoku University, Sendai 980-8577, Japan*

[2]*Spin Quantum Rectification Project, ERATO, Japan Science and Technology Agency, Sendai 980-8577, Japan*

[3]*The Advanced Science Research Center, Japan Atomic Energy Agency, Tokai 319-1195, Japan*

[4]*Department of Applied Physics, Tohoku University, Sendai 980-8579, Japan*

[5]*PRESTO, Japan Science and Technology Agency, Saitama 332-0012, Japan*

[6]*WPI Advanced Institute for Materials Research, Tohoku University, Sendai 980-8577, Japan*

*Electronic address: daichi.kinken@imr.tohoku.ac.jp

†Electronic address: eizi@imr.tohoku.ac.jp

DOI: 10.1038/NPHYS3895

SA. Antiferromagnetic spin-1/2 chain

Here, we shortly review the low-energy properties of one-dimensional (1D) antiferromagnetic (AF) spin-1/2 chains. A typical Hamiltonian of an AF spin-1/2 chain is given by

$$\mathcal{H} = -J\sum_j (S_j^x S_{j+1}^x + S_j^y S_{j+1}^y + \Delta S_j^z S_{j+1}^z) - B\sum_j S_j^z, \tag{S1}$$

where $\boldsymbol{S}_j$ is the spin-1/2 operator on the j-th site (we set $\hbar = 1$), $J < 0$ is the AF exchange coupling, Δ is the Ising-type anisotropy, and $B = g\mu_B H$ is the magnitude of the external magnetic field (g, μ_B, and H are the g factor, the Bohr magneton, and the magnetic field, respectively). Note that $\boldsymbol{S}_j$ is defined as $\boldsymbol{S}_j = -\boldsymbol{S}_j^{\rm e}$ ($\boldsymbol{S}_j^{\rm e}$: electron-spin operator) in Eq. (S1) in accordance with a standard notation. $\Delta = 1$ corresponds to the $SU(2)$-symmetric Heisenberg model. The above model (S1) was found to well describe magnetic properties of actual quasi-one-dimensional cuprates including Sr_2CuO_3.

The low-energy physics of the spin chain is well described by the Tomonaga-Luttinger liquid (TL-liquid) theory [5, 31, 32] with gapless spinon excitations. The Hamiltonian of a TL liquid is equivalent to that of a gapless free boson field theory,

$$\mathcal{H}_{\rm TL} = \int dx \frac{v}{2}\left[\frac{1}{K}(\partial_x\phi)^2 + K(\partial_x\theta)^2\right], \tag{S2}$$

where $\phi(x,t)$ and $\theta(x,t)$ are a pair of real boson fields and satisfy the canonical commutation relation $[\phi(x,t), \partial_{x'}\theta(x',t)] = i\delta(x-x')$ (x and t are the space and time coordinates, respectively); v and K denote the spinon velocity and the TL-liquid parameter, respectively. Through field theory procedures [5], Eq. (S2) is derived from the lattice model of Eq. (S1). Spin operators are expressed by using the fields ϕ and θ, and they describe the spinon dynamics. We note that spinons possess fermionic nature, but spin operators are bosonic since they consist of products of paired spinons. The gapless phase of the Heisenberg model ($\Delta = 1$) is fairly stable against the magnetic field B and the Ising-type anisotropy $|\Delta| < 1$. For example, the gapless excitation survives in the regime from zero field to the saturation field $B_c = 2J$ [5].

SB. Spin Seebeck effect in AF spin-1/2 chains

In this section, we explain a theory of the longitudinal spin Seebeck effect (LSSE) of spin-1/2 AF chains (S1). We consider the model for the experimental set-up (Fig. 1b), as

shown in Fig. S1, where temperatures of the spin chain (Sr_2CuO_3) and the metal (Pt) are respectively set to be T_s and T_m, and the exchange coupling J_{sd} exists at the interface. For this set-up, the microscopic theory [28, 33] based on Keldysh formalism [34, 35] shows that the spin current I_s injected into the metal across the interface is given by

$$I_s = -\frac{2N_{\rm int}J_{\rm sd}^2}{\sqrt{2}\pi}\int_{-\infty}^{\infty} d\omega\ {\rm Im}\chi^{-+}(\omega)\ {\rm Im}X^{-+}(\omega)\ \left[n(T_{\rm m})-n(T_{\rm s})\right] \tag{S3}$$

where χ^{-+} and X^{-+} are, respectively, the local-spin dynamical susceptibilities of the metal and the spin chain, $n(T)=1/(e^{\omega/T}-1)$ is the Bose distribution function (ω: frequency), and $N_{\rm int}$ is the total number of sites at the interface. Indices $-+$ denote the transverse spins $S^{\pm}=S^x\pm iS^y$, and the explicit form of X^{-+} is given by

$$\begin{aligned} X^{-+}(\omega) &= \frac{1}{N}\sum_k X^{-+}(\omega,k), \\ X^{-+}(\omega,k) &= -\int_0^{\beta} d\tau e^{i\omega_n\tau}\sum_j e^{-ikj}\langle T_\tau S_j^-(\tau)S_0^+(0)\rangle\Big|_{i\omega_n\to\omega+i0}, \end{aligned} \tag{S4}$$

where k is the wave number, N is the total number of sites, τ is imaginary time, $\beta=1/T$, $\omega_n=2\pi n/\beta$ (n: integer), and T_τ stands for imaginary-time ordered product. The susceptibility of metal χ^{-+} is also defined by replacing j, k and $S_j^{\pm}$ with conduction electron's coordinate $\boldsymbol{r}$, wave vector $\boldsymbol{k}$ and spins $s_{\boldsymbol{r}}^{\pm}$ in Eq. (S4), respectively. This interface spin current is converted into an electric current in the metal via the inverse spin Hall effect [20−22]; thus the LSSE voltage observed in the present study is proportional to the spin current I_s. Equation (S3) shows that I_s vanishes when the temperature difference $\delta T=T_{\rm s}-T_{\rm m}$ is zero. We emphasize that this spin-current formula using dynamic susceptibilities is applicable to magnetically disordered as well as ordered states.

Here, we comment on effects of Anderson localization. For transport phenomena in low-dimensional systems, effects of disorder such as defects and impurities generally become relevant in a low-energy and low-temperature limit [29, 36, 37]. However, recent experiments on Sr_2CuO_3 [18,19] detected large thermal conductivity conveyed by spinons, showing that at least a part of spinon transport survives free from localization. In addition, exact analysis based on the Bethe ansatz [38] shows that finite Drude weight of thermal conductivity (i.e., ballistic spinon transport) exists in the whole finite-temperature range in the spin-1/2 XXZ chain (S1) with $B\neq 0$. These results imply that coherent spinon transport in Sr_2CuO_3 survives in the temperature range of this work. Therefore, Anderson localization effects may be neglected for a practical approximation when one calculates the interface spin current I_s.

DOI: 10.1038/NPHYS3895

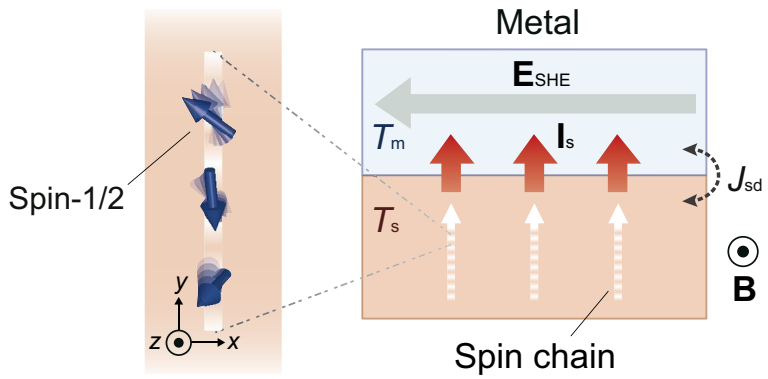

FIG. S1: Model for spin Seebeck effect in one-dimensional spin chains. $T_{\rm m}$ denotes the effective temperature of electrons in the metal; $T_{\rm s}$ that of spinons in the one-dimensional spin chains. The spin current $\mathbf{I}_{\rm s}$ is injected into the metal via the interface exchange interaction with the magnitude $J_{\rm sd}$ under the magnetic field $\mathbf{B}$. $\mathbf{I}_{\rm s}$ is converted into the electromotive force $\mathbf{E}_{\rm SHE}$ via the inverse spin Hall effect.

Let us simplify the spin-current formula (S3). The susceptibility of the metal may be approximated by a spin-diffusion type function $\mathrm{Im}\chi^{-+}(\omega) = \chi_0\omega\tau_s/(1+\tau_s^2\omega^2)$, where χ_0 is the static susceptibility of the metal, and the spin relaxation time τ_s is almost unchanged with changing $T_{\rm m}$ and B [28]. Since $\mathrm{Im}\chi^{-+}$ and the T-dependent factor $n(T_{\rm m}) - n(T_{\rm s})$ are both odd with respect to ω, the formula (S3) shows that the necessary and sufficient condition for generating a finite spin current is to make $\mathrm{Im}X^{-+}$ deviate from the ω-odd function. When $\delta T = T_{\rm s} - T_{\rm m}$ is sufficiently small, $n(T_{\rm m}) - n(T_{\rm s})$ can be approximated by $-\omega\delta T/(4T^2\sinh^2(2\omega/T))$, where $T = (T_{\rm s}-T_{\rm m})/2$. Using these relations of the susceptibility χ^{-+} and the T factor, we can simplify the formula (S3). The normalized spin current $\tilde{I}_s$ defined by $I_s = -\frac{N_{\rm int}J_{\rm sd}^2}{2\sqrt{2}\pi}\tilde{I}_s\delta T$ is given by

$$\tilde{I}_s = \frac{1}{T^2}\int_{-\infty}^{\infty} d\omega\ \mathrm{Im}X^{-+}(\omega)\frac{\omega^2}{1+\tau_s^2\omega^2}\frac{1}{\sinh^2(\omega/(2T))}. \tag{S5}$$

The remaining task is to compute $\mathrm{Im}X^{-+}$ in Eq. (S5). The TL-liquid theory including bosonization [5, 31, 32] and conformal field theory [39] provides a powerful way of calculating dynamical correlation functions of TL-liquid phases, and the results are reliable in the low-energy and low-temperature regime. The most dominant region of the dynamical susceptibility $X^{-+}(\omega,k)$ is located around $k=\pi$ owing to the antiferromagnetic correlation. The other gapless contribution to $X^{-+}(\omega,k)$ appears also around $k = \pm 2\pi M$ ($M = \langle S_j^z\rangle$),

but the magnitude is known to be negligible compared with that around $k = \pi$. According to the TL-liquid theory of Eq. (S2), X^{-+} around $k = \pi$ is computed as [5]

$$X^{-+}_{\rm TL}(\omega, \pi + \delta k) = -B_0^2 \frac{a_0}{v} \sin\Big(\frac{\pi}{2K}\Big)\Big(\frac{2\pi a_0}{\beta v}\Big)^{1/K-2} B\Big(-i\frac{\beta(\omega - v\delta k)}{4\pi} + \frac{1}{4K}, 1 - \frac{1}{2K}\Big) \times B\Big(-i\frac{\beta(\omega + v\delta k)}{4\pi} + \frac{1}{4K}, 1 - \frac{1}{2K}\Big), \quad \text{(S6)}$$

where $B(x, y) = \Gamma(x+y)/(\Gamma(x)\Gamma(y))$ is the Beta function, and B_0 is a non-universal constant. Microscopic information about the original spin chain is included in the parameters v, B_0 and K, which are functions of J, Δ and B. At the $SU(2)$-symmetric Heisenberg point $\Delta = 1$, the value of K monotonically increases from 1 to 2 as the magnetic field B changes from 0 to the saturation value $2J$. Accurate values of v, B_0 and K are listed in Refs. [5, 40–42]. Using them, we obtain the ω-, k-, and T-dependences of the susceptibility X^{-+} from Eq. (S6). The large amplitude of $X^{-+}_{\rm TL}$ appears around the linearized spinon dispersion curve $\omega = \pm v(k - \pi) = \pm v\delta k$, and the spectrum is continuously distributed in (ω, k) space. The continuous spectrum implies the fermionic nature of spinons and the existence of a spinon "Fermi" surface. Equation (S6) shows that ${\rm Im}X^{-+}_{\rm TL}(\omega, k)$ is negative (positive) in the positive-ω (negative-ω) region.

At $B = 0$, ${\rm Im}X^{-+}_{\rm TL}(\omega) = N^{-1}\sum_{\delta k} {\rm Im}X^{-+}_{\rm TL}(\omega, \pi + \delta k) = (2\pi)^{-1}\int_0^{\Lambda} dp\ {\rm Im}X^{-+}_{\rm TL}(\omega, \pi + p)$ is an ω-odd function (Λ: a proper high-energy cut off). Therefore, the spin current vanishes at zero field. This result can be obtained also by using time-reversal or spin-rotational symmetry. However, the formula (S6) also shows that for finite fields $B \neq 0$, ${\rm Im}X^{-+}_{\rm TL}$ is still ω-odd; the spin current is zero even at $B \neq 0$. This suggests that the simple TL-liquid theory with the linear spinon dispersion is not sufficient to explain the LSSE of quantum spin chains. This situation contrasts with the fact that the TL-liquid theory has successfully explained other dynamical phenomena of 1D magnets such as electron spin resonance [43], nuclear magnetic resonance [44–46], and neutron scattering spectra [47–49].

In addition to the TL-liquid theory, other powerful theoretical techniques were developed for 1D quantum many-body systems. The Bethe ansatz [50–52], one of such techniques, is applicable to the AF spin-1/2 chain and it can exactly compute the dynamical correlation functions at $T = 0$. It shows that the *curved* spinon dispersion $\omega = \epsilon(\delta k)$ gives the lower bound of the spectrum ${\rm Im}X^{-+}(\omega, \pi + \delta k)$ around $k = \pi$. This is also supported by numerical calculations [53]. The analytical form of the curved spinon dispersion of the Heisenberg

DOI: 10.1038/NPHYS3895

model ($\Delta = 1$) at $T = 0$ is given by [30]

$$\epsilon(\delta k) \;=\; 2J\left[\frac{\pi}{2}+\frac{B}{2}\left(1-\frac{\pi}{2}\right)\right]\cos\left(\frac{\delta k}{2}\right)\sin\left(\frac{\delta k}{2}+\pi M\right)-B, \tag{S7}$$

where $M = \frac{1}{\pi}\arcsin\left(\frac{1}{1-\pi/2+\pi/B}\right)$ is the uniform magnetization per site $\langle S_j^z\rangle$ at $T = 0$. The dispersion $\epsilon(\delta k)$ converges to the des Cloizeaux-Pearson mode $\frac{\pi}{2}J\sin(\delta k)$ when B is close to zero. On the other hand, in the formula (S6), the spinon dispersion is approximated by the linearized dispersion $\omega = \pm v\delta k$. Because of this linear dispersion, both the positive- and negative-ω weights of Eq. (S6) cancel out. Therefore, a reasonable improvement of Eq. (S6) is to replace the linearized dispersion $\omega \pm v\delta k$ with the curved dispersion $\omega - \epsilon(\pm\delta k)$. This replacement is also justified by a recently developed nonlinear TL-liquid theory [54]. Figure S2 shows that with increasing B (> 0), the curved dispersion $\omega = \epsilon(\delta k)$ becomes the flatter in the positive-ω region than in the negative-ω region. As a result, the contribution from the positive-ω region is dominant in I_s, which means that down-spin spinons are the main carriers of the spin current. We note that up-spin magnons are spin carriers for the LSSE in 3D ordered ferromagnets differently from the case of spinons, as shown below. By substituting $\omega = \epsilon(\delta k)$ in Eq. (S6), we finally obtain negative spin currents for positive external fields $B > 0$. The negative sign is attributed to the dominant, negative weight of $\mathrm{Im}X^{-+}(\omega, k)$ in the positive-ω region, and the sign is opposite to that of spin currents in 3D ordered ferromagnets. This agrees with the experimental result of the main text. Our calculation with the curved dispersion also reproduces the B-linear dependence of I_s in the low-field region ($|B| < J$), as shown in Fig. 4 of the main text. In Fig. 4, keeping the LSSE in Sr_2CuO_3 in mind, we set $J = -2000$ K, $\Delta = 1$, $T = 20$ K and $\tau_s = 1/(200\ \mathrm{K})$ [28]. We emphasize that it is essential to take into account the curved dispersion (i.e., breaking of "particle-hole" symmetry) in calculating the spinon spin Seebeck effect.

SC. Spin Seebeck effect in ferromagnets

In this section, we review the theory of LSSE for three-dimensional (3D) ordered ferromagnetic insulators [28]. We consider a simple Heisenberg ferromagnet on a cubic lattice, whose Hamiltonian is given by

$$\mathcal{H}_{\mathrm{3D}} \;=\; -J\sum_{\langle \boldsymbol{r},\boldsymbol{r}'\rangle}\boldsymbol{S}_{\boldsymbol{r}}\cdot\boldsymbol{S}_{\boldsymbol{r}'} - D_z\sum_{\boldsymbol{r}}(S_{\boldsymbol{r}}^z)^2 - B\sum_{\boldsymbol{r}}S_{\boldsymbol{r}}^z, \tag{S8}$$

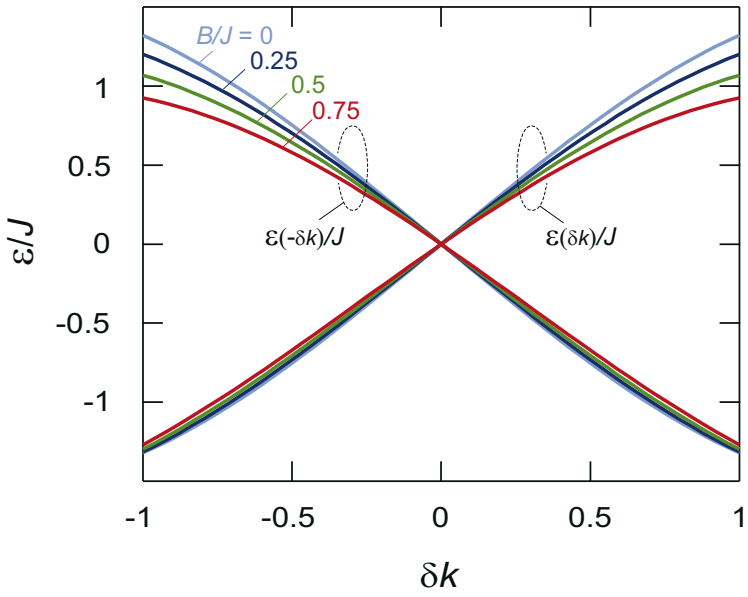

FIG. S2: Curved spinon dispersion $\omega = \epsilon(\pm\delta k)$ as a function of B in the Heisenberg chain $\Delta = 1$.

where $\boldsymbol{S}_{\boldsymbol{r}}$ is the spin-S operator on site $\boldsymbol{r}$, $J > 0$ is the ferromagnetic exchange coupling constant, $D_z > 0$ is the easy-axis anisotropy. Equation (S3) can be used to calculate spin currents for ferromagnets by replacing $N^{-1}\sum_k X^{-+}(\omega, k)$ with the susceptibility of a ferromagnet $(N_x N_y N_z)^{-1}\sum_{\boldsymbol{k}} X^{-+}(\omega, \boldsymbol{k})$ in Eqs. (S3) and (S4) (N_α is the total number of sites along the α direction).

The spin-wave theory [55–57] is useful for computing the susceptibility of ordered ferromagnets in the low-temperature regime ($T < J$). According to the spin-wave theory, the Hamiltonian of Eq. (S8) is approximated by

$$\mathcal{H}_{\rm 3D}^{\rm sw} = \sum_{\boldsymbol{k}} \omega_{\rm sw}(\boldsymbol{k}) a_{\boldsymbol{k}}^\dagger a_{\boldsymbol{k}}, \tag{S9}$$

where $a_{\boldsymbol{k}}^\dagger$ ($a_{\boldsymbol{k}}$) is the creation (annihilation) operator of a magnon with the wave vector $\boldsymbol{k}$, and $\omega_{\rm sw}(\boldsymbol{k}) = -2SJ(\cos k_x + \cos k_y + \cos k_z - 3) + 2SD_z + B$ is the magnon dispersion. Here we have assumed that spins are polarized along the direction of $B > 0$. In the magnon (spin-wave) picture, the transverse spin susceptibility is given by the Green function of magnons

$$X^{-+}(\omega, \boldsymbol{k}) = -\frac{2S}{\omega + \omega_{\rm sw}(\boldsymbol{k}) + i\eta} \tag{S10}$$

with $\eta \to +0$. Accordingly, the imaginary part is ${\rm Im}X^{-+}(\omega, \boldsymbol{k}) = 2\pi S\delta(\omega + \omega_{\rm sw}(\boldsymbol{k}))$. The

DOI: 10.1038/NPHYS3895

temperature effect on the susceptibility can be described by replacing S with $\tilde{S} = S - \langle a^\dagger_{\boldsymbol{r}} a_{\boldsymbol{r}} \rangle$ in Eq. (S10). The calculated susceptibility shows that the weight of $\mathrm{Im}X^{-+}$ is located in the negative-ω region, which contrasts with the spinon case where the $\mathrm{Im}X^{-+}$ in the positive-ω region is dominant. This results in the positive sign of spin current in ferromagnets, which is opposite to that of spin chains. The explicit form of the spin current in a 3D ferromagnet is given by

$$\tilde{I}_s = \frac{\tilde{S}}{T^2} (2\pi)^{-3} \int_{-\pi}^{\pi} dk_x dk_y dk_z \, \frac{\omega_{\mathrm{sw}}(\boldsymbol{k})^2}{1 + \tau_s^2 \omega_{\mathrm{sw}}(\boldsymbol{k})^2} \frac{1}{\sinh^2(2\omega_{\mathrm{sw}}(\boldsymbol{k})/T)}. \tag{S11}$$

In a low-temperature region, the magnon dispersion is approximated by a spherical one $\omega_{\mathrm{sw}}(\boldsymbol{k}) \approx SJ|\boldsymbol{k}|^2 + \epsilon_0$ with the spin gap $\epsilon_0 = 2SD_z + B$. Thus, the multiple integration $(2\pi)^{-3} \int dk_x dk_y dk_z$ is reduced to $(2\pi^2)^{-1} \int_0^{\Lambda'} dk \; k^2$, where Λ' is the high-energy cut off of the magnon energy band. The field dependence of the spin current in Eq. (S11) is shown in Fig. 4 of the main text, in which we set $S = 2$, $J = 50$ K, $D_z = 0.01J$, $T = 20$ K and $\tau_s = 1/(200\ \mathrm{K})$ [28]. The result is consistent with experimental results of ferromagnets such as $Y_3Fe_5O_{12}$ [11, 12, 58].

SD. Spin Seebeck effect in antiferromagnets

In this section, we consider LSSE in 3D ordered AF insulators. A Hamiltonian for antiferromagnets is given by changing the sign of the exchange coupling J in Eq. (S8).

When a simple antiferromagnet is under the magnetic field B (necessary for SSEs), the antiferromagnet is forced into a non-collinear spin configuration [56], shown in Fig. S3. The magnetic structure consists of two sublattices A and B. A uniform magnetization is induced in the field direction by applying the field B and it grows with B, while the components normal to B cancel out on each pair of the A and B sublattices. This AF state is realized in Sr_2CuO_3 in the low-temperature phase at $T < 5$ K in this work.

Because of the field-induced magnetization, up-spin angular momentum is carried by magnons in the AF state similarly to ferromagnetic magnons. Accordingly, the polarization direction of the spin current is the same for the AF state and a ferromagnetic state. We again note that, in a spin-1/2 AF chain, both up- and down-spin spinons are gapless under magnetic fields and thus the curvature of the spinon dispersion determines the sign of spin current.

The positive sign of spin current in the AF ordered state can be formulated from a more microscopic viewpoint as follows. The unit cell of the AF state is a pair of neighboring A and B sublattices, and thus two magnon modes $\epsilon_{\pm}(\boldsymbol{k})$ appear [59], depicted in Fig. S3. $\epsilon_{\pm}(\boldsymbol{k})$ are given by

$$\epsilon_{\pm}(\boldsymbol{k}) = \sqrt{A_{\pm}^2(\boldsymbol{k}) - B^2(\boldsymbol{k})}, \tag{S12}$$

where $A_{\pm}(\boldsymbol{k}) = B\sin\theta + 3SD_z(\sin^2\theta - 1/3) + Sz|J|\cos(2\theta) \mp Sz|J|\gamma_{\boldsymbol{k}}(\cos(2\theta) - 1)/2$, $B(\boldsymbol{k}) = Sz|J|\gamma_{\boldsymbol{k}}(\cos(2\theta) + 1)/2 - SD_z\cos^2\theta$, and D_z is the anisotropy. Here, $z = 6$ is the coordination number, θ is the angle characterizing the spin configuration given by $\sin\theta = B/(2S(z|J| - D_z))$, and $\gamma_{\boldsymbol{k}} = 2z^{-1}\sum_{a=x,y,z}\cos(k_a)$. The gapless Nambu-Goldstone dispersion $\epsilon_{-}(\boldsymbol{k})$ emerges owing to the spontaneous breaking of the $U(1)$ symmetry around the field direction. We note that the edges of the Brillouin zone above the AF ordering are reduced to $\boldsymbol{k} = \boldsymbol{0}$ in the present Brillouin zone for the two-site unit cell; thus the gapless nature of $\epsilon_{-}(\boldsymbol{k})$ around $\boldsymbol{k} = \boldsymbol{0}$ reflects the AF correlation. Calculating with the use of the linear spin-wave theory yields the dynamical susceptibility $X^{-+}(\boldsymbol{k},\omega)$ for spins on each sublattice. The suseptibility of sublattice A is shown to be equal to that of sublattice B, and the imaginary part is given by

$$\begin{aligned}\mathrm{Im}X^{-+}(\boldsymbol{k},\omega) \;=\; & \frac{\pi S}{2}(1+\sin^2\theta)\Big\{\frac{A_{-}(\boldsymbol{k})}{\epsilon_{-}(\boldsymbol{k})}[\delta(\omega+\epsilon_{-}(\boldsymbol{k})) - \delta(\omega-\epsilon_{-}(\boldsymbol{k}))] \\ & + \frac{A_{+}(\boldsymbol{k})}{\epsilon_{+}(\boldsymbol{k})}[\delta(\omega+\epsilon_{+}(\boldsymbol{k})) - \delta(\omega-\epsilon_{+}(\boldsymbol{k}))]\Big\} \\ & + \pi S\sin\theta\Big\{[\delta(\omega+\epsilon_{-}(\boldsymbol{k})) + \delta(\omega-\epsilon_{-}(\boldsymbol{k}))] + [\delta(\omega+\epsilon_{+}(\boldsymbol{k})) + \delta(\omega-\epsilon_{+}(\boldsymbol{k}))]\Big\}.\end{aligned} \tag{S13}$$

This equation shows that both magnon modes contribute to the dynamical susceptibility $X^{-+}(\omega)$ in the spin-current formula (S3). The first and second lines in Eq. (S13) are ω-odd parts, and the third line is an ω-even part; therefore, only the third line gives rise to finite spin current in the spin-current formula (S3). The ω-even part is positive for $B > 0$ and thus leads to the positive sign of spin current, which is the same sign as that in the ferromagnetic LSSE. This means that the negative-ω region is more dominant than the positive-ω region in the spectrum of $\mathrm{Im}X^{-+}(\omega)$. Our calculation is consistent with the experimental result of LSSE in the low-temperature phase of Sr_2CuO_3 at $T < 5$ K. Furthermore, recent experiments [24,60] showed that LSSE voltage in AF insulators is of the same sign as that in ferromagnets.

DOI: 10.1038/NPHYS3895

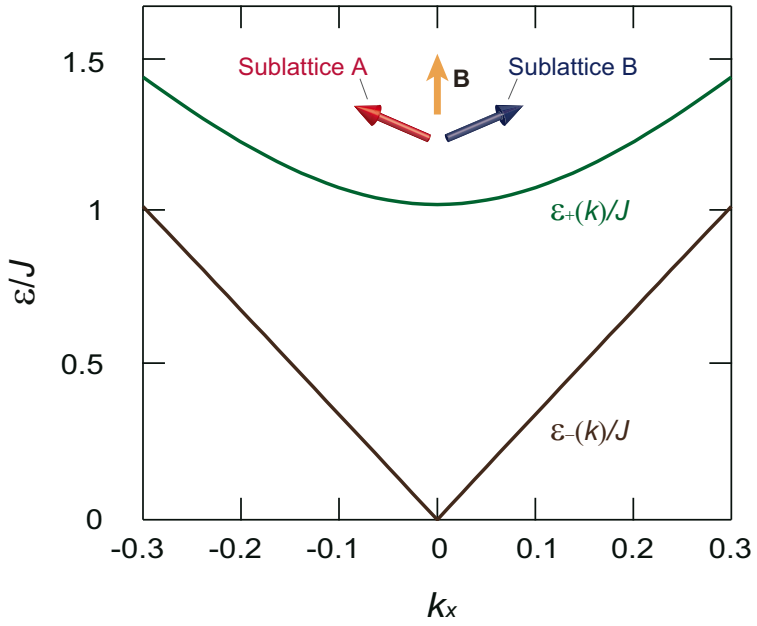

FIG. S3: Two magnon dispersions $\epsilon_{\pm}(\boldsymbol{k})$ near the Γ point, $\boldsymbol{k} = (0, 0, 0)$. The schematic illustration shows a spin configuration in the AF state induced by the external field.

Additional References

[31] Tsvelik, A. M. *Quantum Field Theory in Condensed Matter Physics* (Cambridge Univ. Press, 2007).

[32] Gogolin, A. O., Nersesyan, A. A. & Tsvelik A. M. *Bosonization and Strongly Correlated Systems* (Cambridge Univ. Press, 2004).

[33] Xiao, J., Bauer, G. E. W., Uchida, K., Saitoh, E. & Maekawa, S. *Phys. Rev. B* **81,** 214418 (2010).

[34] Zagoskin, A. *Quantum Theory of Many-Body Systems: Techniques and Applications* (Springer, 2014).

[35] Rammer, J. *Quantum Field Theory of Non-equilibrium States* (Cambridge Univ. Press, 2011).

[36] Kane, C. L. & Fisher, M. P. A. *Phys. Rev. B* **46,** 15233 (1992).

[37] Furusaki, A. & Nagaosa, N. *Phys. Rev. B* **47,** 4631 (1993).

[38] Klümper, A. & Sakai, K. *J. Phys. A* **35,** 2173 (2002).

[39] Francesco, P., Mathieu, P. & Sénéchal, D. *Conformal Field Theory* (Springer, 1999).

[40] Lukyanov, S. & Zamolodchikov, A. *Nucl. Phys. B* **493,** 571 (1997); Lukyanov, S. *Phys. Rev. B* **59,** 11163 (1999); Lukyanov, S. & Terras, V. *Nucl. Phys. B* **654,** 323 (2003).

[41] Hikihara, T. & Furusaki, A. *Phys. Rev. B* **58,** R583 (1998); *Phys. Rev. B* **69,** 064427 (2004).

[42] Takayoshi, S. & Sato, M. *Phys. Rev. B* **82,** 214420 (2010).

[43] Oshikawa, M. & Affleck, I. *Phys. Rev. Lett.* **82,** 5136 (1999); *Phys. Rev. B* **65,** 134410 (2002).

[44] Takigawa, M., Motoyama, N., Eisaki, H. & Uchida, S. *Phys. Rev. Lett.* **76,** 4612 (1996).

[45] Thurber, K. R., Hunt, A. W., Imai, T. & Chou, F. C. *Phys. Rev. Lett.* **87,** 247202 (2001).

[46] Sato, M., Hikihara, T. & Momoi, T. *Phys. Rev. B* **83,** 064405 (2011).

[47] Endoh, Y., Shirane, G., Birgeneau, R. J., Richards, P. M. & Holt, S. L. *Phys. Rev. Lett.* **32,** 170 (1974).

[48] Tennant, D. A., Perring, T. G., Cowley, R. A. & Nagler, S. E. *Phys. Rev. Lett.* **70,** 4003 (1993).

[49] Lake, B., Tennant, D. A., Frost, C. D. & Nagler, S. E. *Nature Mat.* **4,** 329 (2005).

[50] Takahashi, M. *Thermodynamics of One-Dimensional Solvable Models* (Cambridge Univ. 2005).

[51] Caux, J-S., Hagemans, R. & Maillet, J. M. *J. Stat. Phys.* P09003 (2005).

[52] Kohno, M. *Phys. Rev. Lett.* **102,** 037203 (2009).

[53] Ishimura, N. & Shiba, H. *Prog. Theo. Phys.* **57,** 1862 (1977); *Prog. Theo. Phys.* **64,** 479 (1980).

[54] Imambekov, A. & Glazman, L. I. *Phys. Rev. Lett.* **102,** 126405 (2009); *Science* **323,** 228 (2009); Imambekov, A., Schmidt, T. L. & Glazman, L. I. *Rev. Mod. Phys.* **84,** 1253 (2012).

[55] Mattis, D. C. *The Theory of Magnetism Made Simple* (World Scientific, 2006).

[56] Yoshida, K. *Theory of Magnetism* (Springer, 1996).

[57] Kittel, C. *Quantum Theory of Solids* (Wiley, 1987).

[58] Jin, H., Boona, S. R., Yang, Z., Myers, R. C., & Heremans, J. P. *Phys. Rev. B* **92,** 054436 (2015).

[59] Kreisel, A., Sauli, F., Hasselmann, N., & Kopietz, P. *Phys. Rev. B* **78,** 035127 (2008).

[60] Wu, S. M., Zhang, W., KC, A., Borisov, P., Pearson, J. E., Jiang, J. S., Lederman, D., Hoffmann, A. & Bhattacharya, A. *Phys. Rev. Lett.* **116,** 097204 (2016).